

# We are IntechOpen, the world's leading publisher of Open Access books Built by scientists, for scientists

6,900

Open access books available

185,000

International authors and editors

200M

Downloads

Our authors are among the

154

Countries delivered to

TOP 1%

most cited scientists

12.2%

Contributors from top 500 universities



WEB OF SCIENCE™

Selection of our books indexed in the Book Citation Index  
in Web of Science™ Core Collection (BKCI)

Interested in publishing with us?  
Contact [book.department@intechopen.com](mailto:book.department@intechopen.com)

Numbers displayed above are based on latest data collected.  
For more information visit [www.intechopen.com](http://www.intechopen.com)



## Monte Carlo Simulations on Defects in Hard-Sphere Crystals Under Gravity

Atsushi Mori  
The University of Tokushima  
Japan

### 1. Introduction

In 1957 the crystalline phase transition in the hard-sphere system was discovered by a Monte Carlo simulation (Wood & Jacobson, 1957) and a molecular dynamics simulation (Alder & Wainwright, 1957). The results of their researches were surprising because the phase transition occurred despite the absence of attractive interparticle interaction. The crystalline phase transition in the hard-sphere system is sometimes referred to as the Alder transition or the Kirkwood-Alder-Wainwright transition. Nowadays, the Alder transition can be interpreted as the competition between two entropic effects; if the configurational entropy overcomes the vibrational one, a disordered fluid phase appears as the stable phase and vice versa. The phase diagram was determined in 1968 by a Monte Carlo simulation (Hoover & Ree, 1968). It is temperature-independent and the phase transition from a disordered fluid phase to a crystalline phase of the face-centered cubic (fcc) structure occurs via a fluid-crystal coexistence region  $\phi_f < \phi < \phi_s$ . Here, the density is expressed by the volume fraction of the hard spheres,  $\phi \equiv (\pi/6)\sigma^3(N/V)$  with  $\sigma$  being the hard-sphere diameter,  $N$  the number of particles, and  $V$  the volume of the system. The Hoover and Ree's values ( $\phi_f = 0.494$  and  $\phi_s = 0.545$ ) have been revised by a direct crystal-fluid coexistence simulation (Davidchack & Laird, 1998) to be  $\phi_f = 0.491$  and  $\phi_s = 0.542$  as extending Mori et al.'s molecular dynamics simulation (Mori et al., 1995).

In 1960-70s colloidal crystallizations were extensively studied as the Alder transitions in reality. Indeed, an effective hard-sphere model successfully explained the colloidal crystal phase transition (Wadachi & Toda, 1972). The recent situation of studies on the colloidal crystal is different from that in those days; so-called hard-sphere suspensions are synthesized (Antl et al., 1986), which exhibit a hard-sphere nature in the crystal-fluid phase transition (Paulin & Ackerson, 1990; Phan et al., 1996; Pusey & van Megen, 1986; Underwood et al., 1994). There is another trend of studies of the colloidal crystals in recent days. Because in the colloidal crystals a periodic structure of dielectric constant with the periodicity of the same order of optical wavelength, the colloidal crystals can be used as photonic crystals. Ohtaka first pointed out this possibility (Ohtaka, 1979). Two 1987 papers triggered this trend (John, 1987; Yablonovitch, 1987). As compared to micro manufacturing technologies of fabricating the photonic crystals, the colloidal crystallization is of low cost in introducing equipment and less time consuming in the fabrication. One of shortcomings of the colloidal crystallization is that the colloidal crystals contain many crystal defects. From fundamental as well as application point of view,

the defect in the photonic crystal should be reduced. For example, the photonic band cannot be opened unless the defect is reduced.

In relation to the reduction of the crystal defects in the colloidal crystals, in 1997 Zhu et al. (Zhu et al., 1986) found an effect of gravity that reduces the stacking disorder in the hard-sphere colloidal crystals. They found that a random hexagonal close pack (rhcp) structure formed under micro gravity. On the other hand, the sediment is rhcp/fcc mixture under normal gravity (Pusey et al., 1989). The mechanism of reduction of the stacking disorder under gravity was so far unresolved until the present author and coworkers found a glide mechanism of disappearance of a stacking fault (Mori et al., 2007a). Viewing  $\langle 111 \rangle$  fcc is characterized by a stacking of ABCABC... sequence, where A, B, and C distinguish hexagonal planes on the basis of the position of the particles within the hexagonal plane. On the other hand, hexagonal close pack (hcp) structure is given by ABAB... stacking and rhcp by a random sequence of A, B, and C. The stacking disorder is the disorder in the sequence of A, B, and C. For example, an intrinsic stacking fault is given by a sequence such as ABABC...; here the third C plane has been removed from ABCABC... We note that even though the stacking is out of order, the particle density remains unchanged. In this respect, the varieties of stacking sequence are not affected by gravity. Thus, the mechanism of the reduction of the stacking disorder due to gravity was a long standing problem. To resolve this problem is the purpose of studies (Mori et al., 2006a;b; 2007a;b; 2009; Mori & Suzuki, 2010; Yanagiya et al., 2005) reviewed in section 4.1.

In a previous paper (Mori et al., 2007a) looking into the evolution of snapshots of Monte Carlo simulations of hard spheres (Mori et al., 2006b), in which transformation from a defective crystal into a less-defective crystal under gravity was observed, we found that a glide of a Shockley partial dislocation terminating an intrinsic stacking fault shrunk the stacking fault in fcc (001) stacking. The key is the fcc (001) stacking; in those simulations this stacking was forced due to a stress from a small periodic boundary simulation box. In contrast, in the colloidal crystallization a patterned bottom wall is sometimes used recently; the fcc (001) stacking is forced due to the stress from the pattern on the bottom. Use of a patterned bottom wall is called a colloidal epitaxy. In 1997 van Blaaderen et al. succeeded in the fcc (001) stacking using a fcc (001) pattern (van Blaaderen et al., 1997). The basic idea of the colloidal epitaxy is that the stacking sequence is unique in  $\langle 001 \rangle$ . The finding of a previous paper (Mori et al., 2007a) is that in the fcc (001) stacking, even if an intrinsic stacking fault running along oblique  $\{111\}$  plane is introduced, through the glide of a Shockley partial dislocation terminating the lower end of the stacking fault the stacking fault shrinks. In other words, their paper points out superiority of the colloidal epitaxy other than the unique stacking sequence. We note here that this glide mechanism is merely one of mechanism. The intrinsic stacking fault is mere one of metastable configurations. Moreover, we have already found a configuration which was succeeded into a newly grown crystal in the fluid phase in some simulation of the same condition (Mori et al., 2007b). An additional remark is that a coherent growth occurred in those simulations (Mori et al., 2006a). Complementarily to the simulations, we have given elastic energy calculations to understand the driving force of upward move of the Shockley partial dislocation (Mori et al., 2009; Mori & Suzuki, 2010).

We note again that in those simulations (Mori et al., 2006a;b; 2007a;b; Yanagiya et al., 2005), fcc (001) stacking was forced due to the stress from a small periodic boundary simulation box. This artifact has been resolved (Mori, in press). The same stress in those previous simulations can, in principle, be provided by the use of patterned substrate (the colloidal epitaxy). However, the system size cannot be systematically enlarged in those simulations

with the flat bottom wall. As already shown (Mori et al., 2006b), fcc {111} stacking occurs for a large lateral system size. In a recent paper (Mori, in press) the square pattern has been used. An advantage of the square pattern is that matching between the crystal grown and the substrate on the lattice line, not only on the lattice point, is possible (Lin et al., 2000). To resolve this shortcoming is the purpose of section 4.2.

The remainder of this chapter is organized as follows. In section 2 remarks on statistical mechanics of the hard-sphere system is described. Simulation method is reviewed in section 3. Results for flat bottom walls are reproduced and discussions for them are given in section 4.1 and some results and discussions for square patterned wall are presented in section 4.2. Conclusions and remarks are given in section 5.

## 2. Hard sphere system

The hard sphere system is comprised of the hard-sphere potential

$$V^{\text{HS}}(r_{ij}) = \begin{cases} \infty & r_{ij} \leq \sigma \\ 0 & r_{ij} > \sigma \end{cases}. \quad (1)$$

Here,  $r_{ij}$  is the interparticle separation between particles  $i$  and  $j$ . The total system energy is given by summing  $V_{ij} \equiv V(r_{ij})$  as

$$U = \sum_{(i,j)} V_{ij}, \quad (2)$$

where the summation is taken for all pairs. The configurational integral is defined as

$$\begin{aligned} Z &= \int \cdots \int dr_1 \cdots dr_N \exp[-U/k_B T], \\ &= \int \cdots \int dr_1 \cdots dr_N \prod_{(i,j)} \exp[-V_{ij}/k_B T], \end{aligned} \quad (3)$$

where  $k_B T$  is the temperature multiplied by Boltzmann's constant. In the integrand, by substituting  $V_{ij}^{\text{HS}}$  [Equation (1)] for  $V_{ij}$ , the quantity  $\exp[-V_{ij}/k_B T]$  takes either 0 or 1.

$$\exp[-V_{ij}/k_B T] = \begin{cases} 0 & r_{ij} \leq \sigma \\ 1 & r_{ij} > \sigma \end{cases}. \quad (4)$$

A special remark is that the commutation of the thermodynamic limit,  $N \rightarrow \infty$  with  $N/V$  kept a finite value, and the hard-sphere limit,  $V_{ij} \rightarrow V_{ij}^{\text{HS}}$ , is not guaranteed. After calculating the probability distribution using a continuum potential  $V_{ij}$  and then taking the hard-sphere limit is not appropriate. Thus, the probability distribution is no longer a continuum function. Monte Carlo simulations are, thus, performed on the basis of equation (4). That is, if any pairs of particle overlap after a Monte Carlo move, then the attempt configuration is rejected, and otherwise accepted. The interaction between a particle and vessel walls is treated in the same manner if the walls are hard bodies.

The present system is exerted to the gravitational field. Thus, the gravitational energy

$$U^g = \sum_{i=1}^N mgz_i, \quad (5)$$

is added to the hard-sphere interaction. Here,  $z_i$  is the  $z$ -coordinate of particle  $i$ . In equation (3),  $U$  is replaced with  $U^{\text{HS}} + U^g$ .

$$Z = \int \cdots \int d\mathbf{r}_1 \cdots d\mathbf{r}_N \prod_{ij} \exp \left[ -\frac{V_{ij}^{\text{HS}}}{k_B T} \right] \prod_k \exp \left[ -\frac{mg\sigma}{k_B T} \frac{z_k}{\sigma} \right]. \quad (6)$$

Here, the dimensionless quantity  $mg\sigma/k_B T \equiv g^*$ , which plays a central role in the hard-sphere system under gravity, is referred to as the gravitational number or the gravitational constant. Accordingly, the attempt configuration after a Monte Carlo move of a particle  $k$  from  $\mathbf{r}_k \equiv (x_k, y_k, z_k)$  to  $\mathbf{r}_k + \Delta\mathbf{r} \equiv (x_k + \Delta x, y_k + \Delta y, z_k + \Delta z)$  is accepted with the probability

$$\exp[-g^* \Delta z^*], \quad (7)$$

in a usual manner, such as Metropolis' method, unless the overlap between particle  $k$  and any other ones occurred. Here,  $\Delta z^* \equiv \Delta z/\sigma$  is the change in  $z$  coordinate of particle  $k$  in unit of length of  $\sigma$  (hereafter, \* indicates this reduced unit).

### 3. Simulation method

#### 3.1 Stepwise control of the gravitational number

In a gravitational sedimentation the gravitational number  $g^*$  is controlled through the temperature  $T$ . In the previous work (Mori et al., 2006b) we proposed the stepwise control of  $g^*$  in order to avoid trapping of the system in a metastable configuration such as a polycrystalline state. Indeed, if  $g^*$  such as  $g^* \geq 0.9$  was turned on from the beginning, the system polycrystallized (Yanagiya et al., 2005). The basic idea of the stepwise  $g^*$  control is that in the simulated tempering (Lyubartev et al., 1992; Marinari & Parizi, 1992), unlike the simulated annealing (Kirkpatrick et al., 1983), no bias of lowering the temperature exists. We considered that if the system was relaxed with no such bias, the trapping into a metastable state such as a polycrystalline state might be avoided.

We note here that  $g^*$  can be controlled more effectively in centrifugation sedimentation of a colloidal dispersion. In the centrifugation method of the colloidal crystallization, such as done previously (Ackerson, 1999; Megens et al., 1997; Suzuki et al., 2007),  $g$  in  $g^* \equiv mg\sigma/k_B T$  can be directly controlled. Taking into account the fact that by the stepwise  $g^*$  control we could successfully avoid the trapping into a metastable state such as a polycrystalline state, a stepwise control of the centrifugation rotation velocity, or a more sophisticated control, must bring a effective control of the crystal defects in the colloidal crystals.

In this chapter, we reproduce results obtained by stepwise  $g^*$  control and will not presented results for simulations with sudden switch-on of gravity. For flat wall simulation (section 4.1) we kept  $g^*$  at a certain value for  $\Delta t = 2 \times 10^5$  Monte Carlo cycles and then increased by  $\Delta g^* = 0.1$ . Here, one Monte Carlo cycle is defined as it contains  $N$  Monte Carlo particle moves. That is, during one Monte Carlo cycle one Monte Carlo particle move is attempted per one particle on average. For square patterned wall simulations (section 4.2) we report results for  $\Delta t = 2 \times 10^5$  Monte Carlo cycles for  $N = 6656$  and  $\Delta t = 8 \times 10^5$  Monte Carlo cycles for  $N = 26624$ .  $\Delta g^* = 0.1$  for both system sizes.

#### 3.2 System size and configuration

In section 4.1 we reproduce results of Monte Carlo simulations of  $N = 1664$  hard spheres in a system with  $L_x^* = L_y^* = 6.27$  and  $L_z^* = 49.23$  (Mori et al., 2006b; 2007a). Flat hard walls were located at  $z = 0$  and  $L_z$ .

After a random initial configuration at  $g^* = 0$  was prepared,  $g^*$  was increased as mentioned in section 3.1. We note that  $\phi = 0.45$  for this system was lower than  $\phi_f$ .  $L_z$  was enough large so that at  $g^*$  where the defect disappearance was observed a vacuum formed on the top. In horizontal ( $x$  and  $y$ ) directions the periodic boundary condition was imposed. In section 4.2 we report the results of Monte Carlo simulations of  $N = 6656$  and  $26624$  systems. The former is four times larger than  $N = 1664$ . Both  $L_x$  and  $L_y$  were doubled, i.e.,  $L_x^* = L_y^* = 12.55$ . The latter is four times larger than  $N = 6656$ ;  $L_x^* = L_y^* = 25.09$ . For both systems we set  $L_z^* = 200$  because volume of the vacuum region on the top of the system do not give affect to the crystal formed at the bottom if the vacuum region is enough large. There is an advantage in preparing a random initial configuration in a case of large  $L_z$ ; we should pay a spatial attention regarding surface ordering on the bottom and top walls and remnant of the crystalline order of the starting configuration if  $L_z$  is small. As for the flat wall case the periodic boundary condition was imposed in horizontal directions. A square patterned hard wall was put at  $z = 0$  and a flat hard wall at  $z = L_z$ . The square pattern is as illustrated in Figure 1. A grid made of square grooves with width  $0.70710678\sigma$  was formed. The diagonal distance of intersections of the longitudinal and transverse grooves was  $0.70710678\sigma \times \sqrt{2} = 0.9999999997\sigma$ . Thus, a hard sphere located on the lattice point of the bottom square lattice can fall into the intersection of the grooves, at most, by almost the half of the hard-sphere diameter; it means that the hard sphere cannot fall on to the bottom of the groove even if the groove depth is larger than  $0.5\sigma$ . The distance between edges of neighboring grooves was  $0.338\sigma$ .

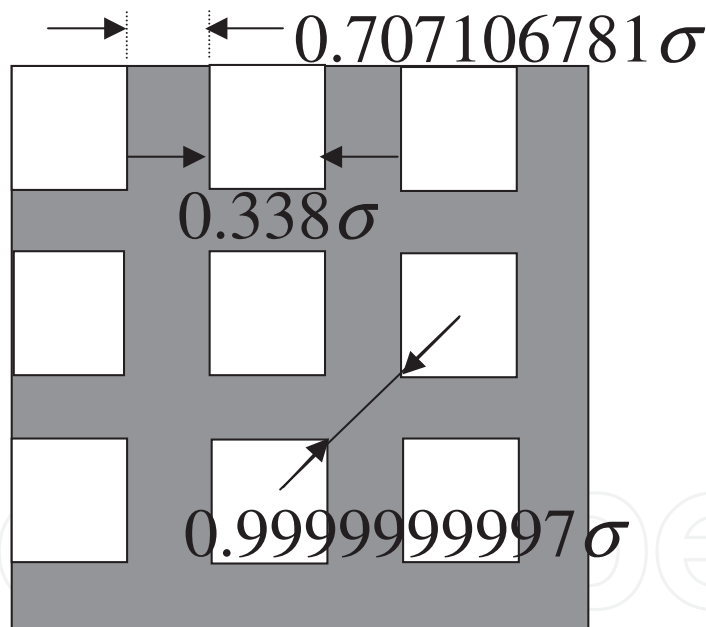


Fig. 1. Illustration of square pattern on the bottom wall.

## 4. Results and discussions

### 4.1 Flat wall case

We plot snapshots projected on  $xz$  plane for the flat bottom wall case in Figure 2. At  $g^* = 0.1$  the system was disordered except for the bottom crystalline layers [Figure 2(a)]. At  $g^* = 0.5$  a defective crystal was formed on the bottom and fluid phase above it [Figure 2(b)]. At  $g^* = 0.9, 1.3,$  and  $1.5$  we find a less-defective crystal on the bottom, a defective crystal above it, and

a fluid phase above the defective crystal [Figure 2(c-e)]. Comparing Figure 2 (c) and (d) we find that the boundary between the less-defective and defective crystals moved upward. Also the top of the defective crystal moved upward. On the other hand, comparing Figure 2 (d) and (e) we find that both the boundary between less-defective and defective crystals and the top of the defective crystal almost remained unchanged. Comparing Figure 2 (c)-(e) we find that the top of the fluid phase lowered with  $g^*$ . We can say that at  $g^* \sim 0.9$ , that is, when the gravitational energy  $mg\sigma$  was comparable to the thermal energy  $k_B T$ , the defect appearance occurred.

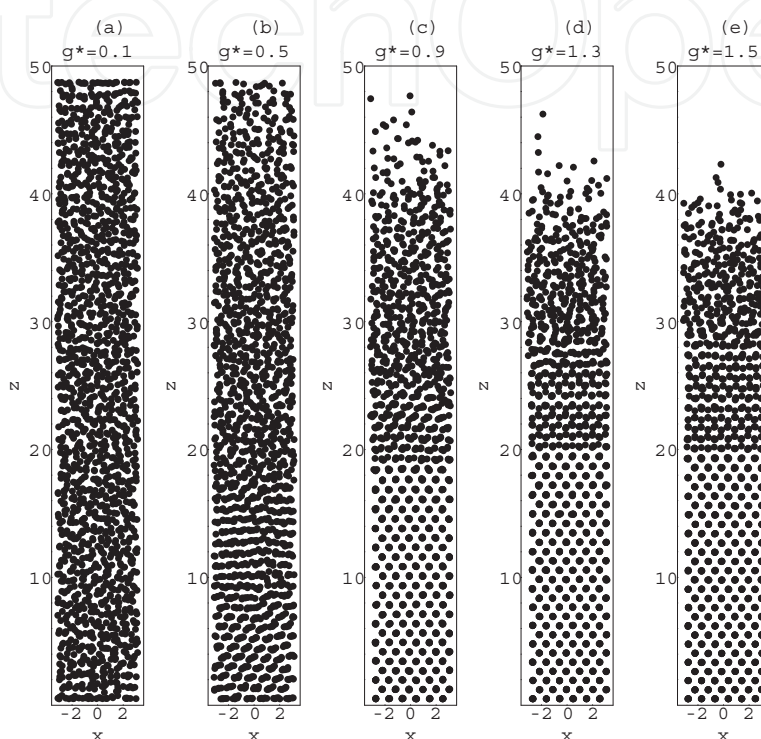


Fig. 2. Projections of snapshots for hard spheres in a system with flat wall; at (a)  $g^* = 0.1$ , (b) 0.5, (c) 0.9, (d) 1.3, and (e) 1.5. Snapshots at the end of duration while  $g^*$  was kept at the value indicated on the top of each figure were plotted. Reprinted with permission from THE JOURNAL OF CHEMICAL PHYSICS 124, 174507 (2006). Copyright 2006, American Institute of Physics.

Before looking into a detail of the process of the defect disappearance, let us note that six crystalline layers exist along  $x$  and  $y$  axes, although  $L_x = L_y$  are four times the fcc lattice constant of the hard-sphere crystal at the crystal-fluid equilibrium. Moreover,  $[100]$  and  $[010]$  are no longer parallel to  $x$  and  $y$  axes, respectively. By a close look, it is found that  $x$  and  $y$  directions are, respectively, parallel to  $[110]$  and  $[\bar{1}\bar{1}0]$ . It means that the pressure at the bottom was higher than that at the crystal-fluid equilibrium. In a mechanical equilibrium

$$\frac{\partial P}{\partial z} = -mg\rho(z), \quad (8)$$

holds, where  $P(z)$  is the pressure at the altitude  $z$  and  $\rho(z)$  the coarse-scale number density at  $z$ . We can understand the higher pressure at the bottom according to this equation. If the relation between  $P$  and  $\rho$  (i.e., the equation of state) is known, we can solve equation (8) with

the condition

$$\int_{-L_x/2}^{L_x/2} \int_{-L_y/2}^{L_y/2} \int_0^{L_z} \rho dx dy dz = N, \quad (9)$$

such as done previously (Biben et al., 1993). Without doing so, we can understand the high pressure through an inequality of thermodynamic stability  $\partial P / \partial \rho > 0$ .

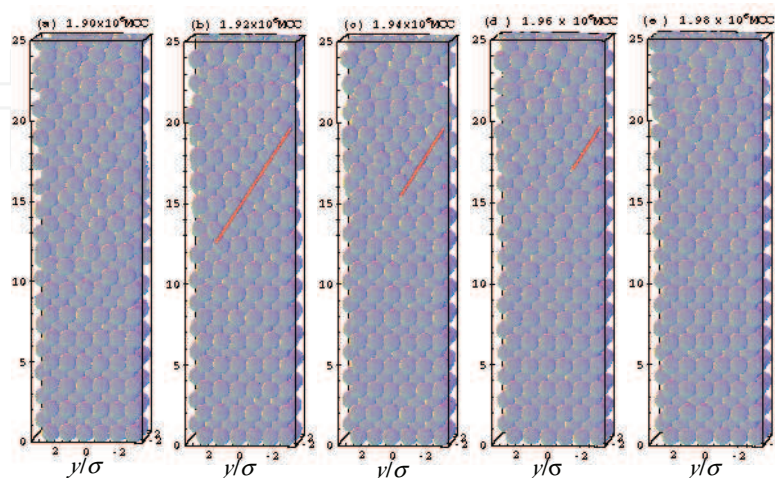


Fig. 3. 3D snapshots during defect disappearance occurred ( $g^* = 0.9$ ) for hard spheres in a system with flat wall; at (a)  $1.99$ , (b)  $1.92$ , (c)  $1.94$ , (d)  $1.96$ , and (e)  $1.97 \times 10^6$  Monte Carlo cycle. Reprinted with permission from *Molecular Physics*, Vol. 105, No. 10, 20 May 2007, 1377–1383. Copyright 2007, Taylor & Francis.

Let us look into the process of the defect disappearance. In Figure 3 evolution of the configuration during  $g^* = 0.9$  is shown in 3D. First of all, we notice that vertical stacking is basically two-fold, indicating the fcc (001) stacking; if the vertical stacking is fcc (111), it is three-fold, namely, ABC... This characteristic can be observed in Figure 2, too.

An intrinsic stacking fault is marked by a red line (an evidence that this defect is an intrinsic stacking fault will be given later). We see that the intrinsic stacking fault is shrinking in the course of the simulation. The altitude of the lower end of the stacking fault coincides with the  $z$  coordinate of the boundary of the less-defective and the defective crystals. We find that the transformation from defective crystal into the less-defective one observed in the two-dimensional snapshots (Figure 2) is accomplished by the shrinking of an intrinsic stacking fault. We note that if we used a different random number in a Monte Carlo simulation the position and the direction of the stacking fault were changed.

The evolution of the center of gravity during  $g^* = 0.9$  is plotted in Figure 4. The center of gravity moved downward overall as the simulation proceeded. Sinking of the center of gravity is understood by taking into account the particle deficiency of the dislocation core located at the lower end of the stacking fault. As the core moves upward the center of gravity sinks. We see plateaus during  $1.84$ - $1.9$  and  $1.96$ - $2 \times 10^6$  Monte Carlo cycles. This means that the system was trapped into metastable configurations during those durations. If the dislocation core goes up and enters into the fluid region, sinking of the center of gravity finishes. The dislocation core in Figure 3 have not gone and not yet entered into the fluid region. So, if we continue the simulation longer than  $2 \times 10^5$  Monte Carlo cycles, further sinking of the center of gravity is expected. It is suggested that the defect disappearance in this case proceeded with temporal trapping by a metastable configuration, though we have not looked into the metastable configuration in the particle level yet.

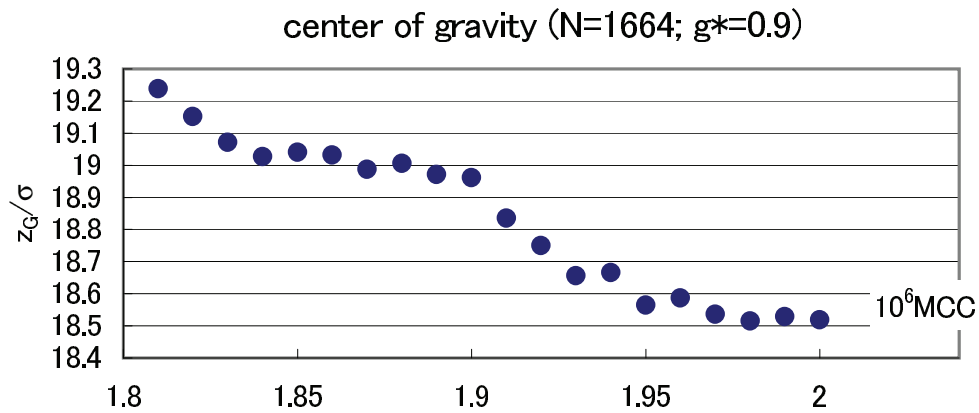


Fig. 4. Evolution of the center of gravity for hard spheres in a system with flat wall during  $g^* = 0.9$ . The centers of gravity are calculated at instant at every  $10^4$  Monte Carlo cycle. Reprinted with permission from Molecular Physics, Vol. 105, No. 10, 20 May 2007, 1377–1383. Copyright 2007, Taylor & Francis.

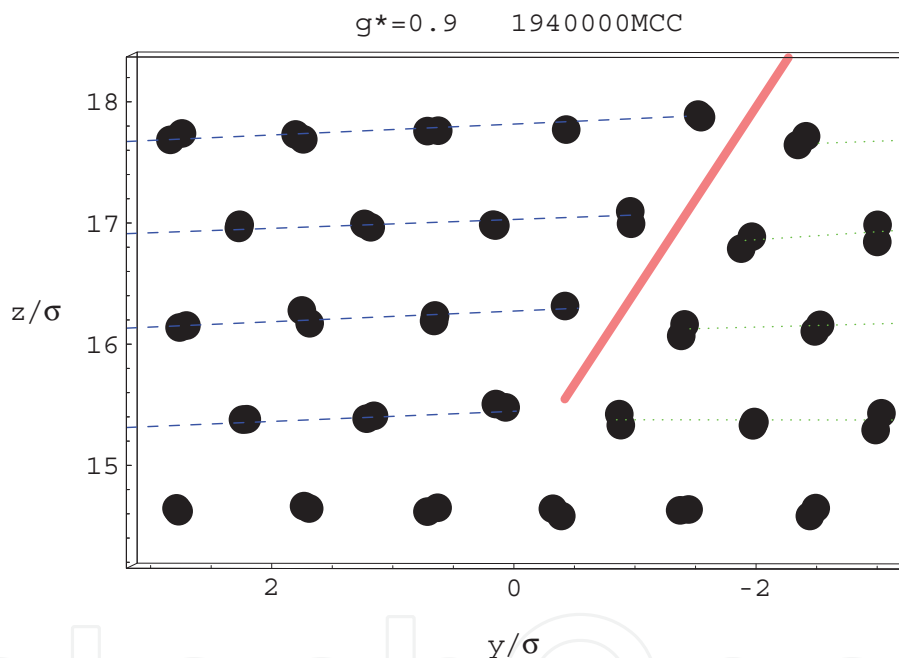


Fig. 5. Magnified snapshot of a defect for hard spheres in a system with flat wall (at  $1.94 \times 10^6$  Monte Carlo cycle). Reprinted with permission from Molecular Physics, Vol. 105, No. 10, 20 May 2007, 1377–1383. Copyright 2007, Taylor & Francis.

An evidence that the defect appearing in Figure 3 is an intrinsic stacking fault with a Shockley partial dislocation terminating its lower end can be given by looking into a magnified snapshot around the lower end of the defect. Figure 5 is a magnified snapshot around a lower end of the defect. The bottom layer includes no fault. The second and above layers include a fault, which is marked by a red line. We note that this fault is parallel to (111). The region up-left of this fault is shifted by  $b^I = (1/6)[211] \equiv a_1/3 + a_2/6 + a_2/6$ , where  $a_1$ ,  $a_2$ , and  $a_2$  are the three lattice vectors.  $b^I$  is the Burgers vector of a Shockley partial dislocation. Accordingly, at the lower end of the fault marked in Figure 5 a Shockley partial dislocation is formed. Because  $b^I$  is the vector connecting a mid point of a upper triangle in

(111) triangular lattice (say, point B) to a mid point of the adjacent lower triangle in (111) lattice (say, point C), the stacking sequence around the fault is ABABC... or equivalent to this. In other words, removing the third C plane from ABCABC... is equivalent to shifting all planes right from the third C plane by  $b^I$ . In this way, the fault marked in Figure 5 is shown to be an intrinsic stacking fault. In a previous paper (Mori et al., 2007a), further, we observed shifts of magnitude of, respectively,  $a/2\sqrt{2}$ ,  $a/6\sqrt{2}$ , and  $a/6$  along  $[110]$ ,  $[\bar{1}10]$ , and  $[001]$ . Here,  $a$  is the fcc lattice constant. Readers may read a monograph (Hirth & Lothe, 1982) for learning the crystallography of defects.

#### 4.2 Squared patterned wall case

We have performed seven Monte Carlo simulations for  $N = 6656$  system and three for  $N = 26624$  with different random numbers. In two of these for  $N = 6656$  defect disappearance at  $g^*$  less than 0.9 was observed. Remember that the defect disappearance occurred during  $g^* = 0.9$  for the flat wall case (Mori et al., 2007a). In four of these for  $N = 6656$  the defect disappearance occurred at  $g^*$  greater than 0.9. For remainder one the defect disappearance was not appreciable. For  $N = 26624$  the defect disappearance occurred at  $g^*$  less than 0.9 for all three cases. In two of three the defect disappearance occurred during  $g^* = 0.5$  and in the remainder one during  $g^* = 0.7$ . The results below are essentially the same as a recent paper (Mori, in press).

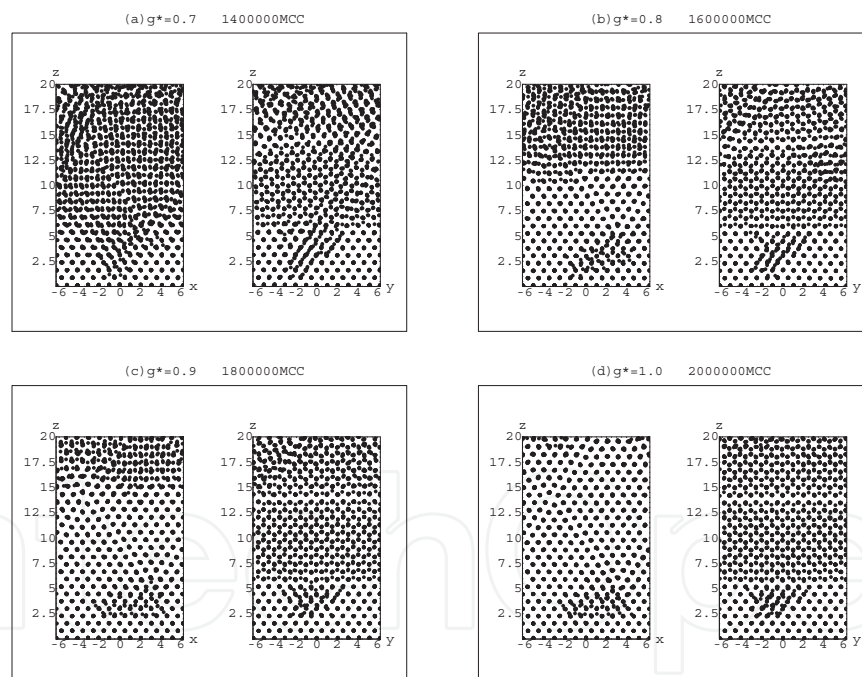


Fig. 6. Snapshot for 6656 hard spheres in a system with the square-patterned wall for a case that defect disappearance occurred at  $g^*$  lower than 0.9; at (a)  $g^* = 0.7$ , (b) 0.8, (c) 0.9, and (e) 1.0.

Figure 6 shows snapshots at  $g^* = 0.7-1.0$  for  $N = 6656$  system for a case that defect disappearance occurred at  $g^*$  less than 0.9. The random number for this simulation is different from that in a recent paper (Mori, in press). Throughout this section the random numbers for reported simulations are different from those in that paper. Though defects in lower portion remained, a defect in appearance expanded over the middle portion disappeared during  $g^* =$

1.0 again. In fcc (001) stacking, if a single stacking fault runs along one of  $\{111\}$  planes,  $[110]$  or  $[\bar{1}\bar{1}0]$  lattice line makes an array of two separated points in a projection on to (110) or  $(\bar{1}\bar{1}0)$ . And, on the other projection we can observe a fault directly. To understand Figure 6 we must take into account the fact that the  $x$  and  $y$  direction correspond to  $[110]$  and  $[\bar{1}\bar{1}0]$ , respectively (Mori et al., 2006b). In Figure 6 (a) splitting is observed in both  $xz$  and  $yz$  projections. Only the splitting in  $xz$  projection in portion  $7 < z^* < 11$  disappeared in Figure 6 (b). Also, the splitting in  $xz$  projection in portion  $z^* > 15$  in Figure 6 (c) disappeared in Figure 6 (d). We conjecture that two stacking faults such as along (111) and  $(\bar{1}\bar{1}\bar{1})$ , not (111) and  $(1\bar{1}\bar{1})$ , coexisted and then that along (111) shrunk. Splitting in both (110) and  $(\bar{1}\bar{1}0)$  is seen in a case that two stacking faults such as along (111) and  $(\bar{1}\bar{1}\bar{1})$  coexist. Making three-dimensional snapshot to observe intersections between (110) or  $(\bar{1}\bar{1}0)$  may give an direct answer to this conjecture. The surface structure of the 3D snapshots was, however, so complicated that we could not follow the edges of the stacking faults although we saw crossing two faults. We left these observations as a future research. Disappearance of only one of projections of lattice lines means the disappearance of the fault in corresponding direction and remaining of the fault in the other direction. There appear defects expanded in a lower-mid region, which remained stably throughout. We see an upper triangular shape at its right in  $xz$  projection and a lower triangular shape at its middle in  $yz$  projection. Upward and downward triangular shapes in projections imply the stacking fault tetrahedra. In (001) stacking, a tetrahedron surrounded by  $\{111\}$  makes upward and downward triangles in projections on to  $[110]$  and  $[\bar{1}\bar{1}0]$ , respectively. Identification of tetrahedra by observing the snapshot layer by layer traversing  $[001]$  is left for a future subject. The stacking fault tetrahedra are suggested to be sessile.

The evolutions of the center of gravity for  $N = 6656$  system during  $g^* = 0.8$  and 1.0 are plotted in Figure 7 for a case that defect disappearance occurred at  $g^*$  lower than 0.9. During  $g^* = 0.8$  [Figure 7 (a)] the relaxation is of a single mode and has not reached to equilibrium yet. Figure 7 (a) is essentially the same as the corresponding figure in a recent paper (Mori, in press). Despite that the defect disappearance was proceeded, the system was not trapped into any metastable configuration. During  $g^* = 1.0$  [Figure 7 (b)], after a first relaxation, sinking of the center of gravity was slowed and then reached to equilibrium. The fluctuation after slowing (during  $1.87\text{-}1.9 \times 10^6$  Monte Carlo cycle) may be fluctuation around a metastable equilibrium. Sinking of the center of gravity in this duration might undergo a temporal stop as for the case of flat bottom wall. Those behaviors are observed in the corresponding figure in a recent paper (Mori, in press). Also, observation of metastable configuration in the particle level has not yet done.

Figure 8 shows snapshots at  $g^* = 0.7\text{-}1.0$  and  $1.3\text{-}1.4$  for  $N = 6656$  system for a case that defect disappearance occurred at  $g^*$  greater than 0.9. We confirm no defect disappearance in Figure 8 (a)-(d). On the other hand, comparing Figure 8 (e) and (f) we find the defect disappearance in  $yz$  projection. The defect disappearance occurred during  $g^* = 1.4$  for this case is vary similar to that observed in Figure 6. What is suggested is essentially the same. The splitting of projection of lattice lines on  $yz$  direction disappeared during  $g^* = 1.4$ . This behavior is exactly the same as that reported in a recent paper (Mori, in press) except for the direction of the fault. Existence of a planner defect in the less defective portion  $z^* < 10$ , which seems as a line in projection, is observed in  $yz$  projection of Figure 8 (f) and  $xz$  projection of the corresponding figure in a recent paper (Mori, in press).

The evolutions of the center of gravity for  $N = 6656$  system during  $g^* = 1.0$  and 1.4 are plotted in Figure 9 for a case that defect disappearance occurred at  $g^*$  lower than 0.9. That during  $g^* = 0.8$  essentially the same as Figure 7 (a) including the statistical error. We may regard the

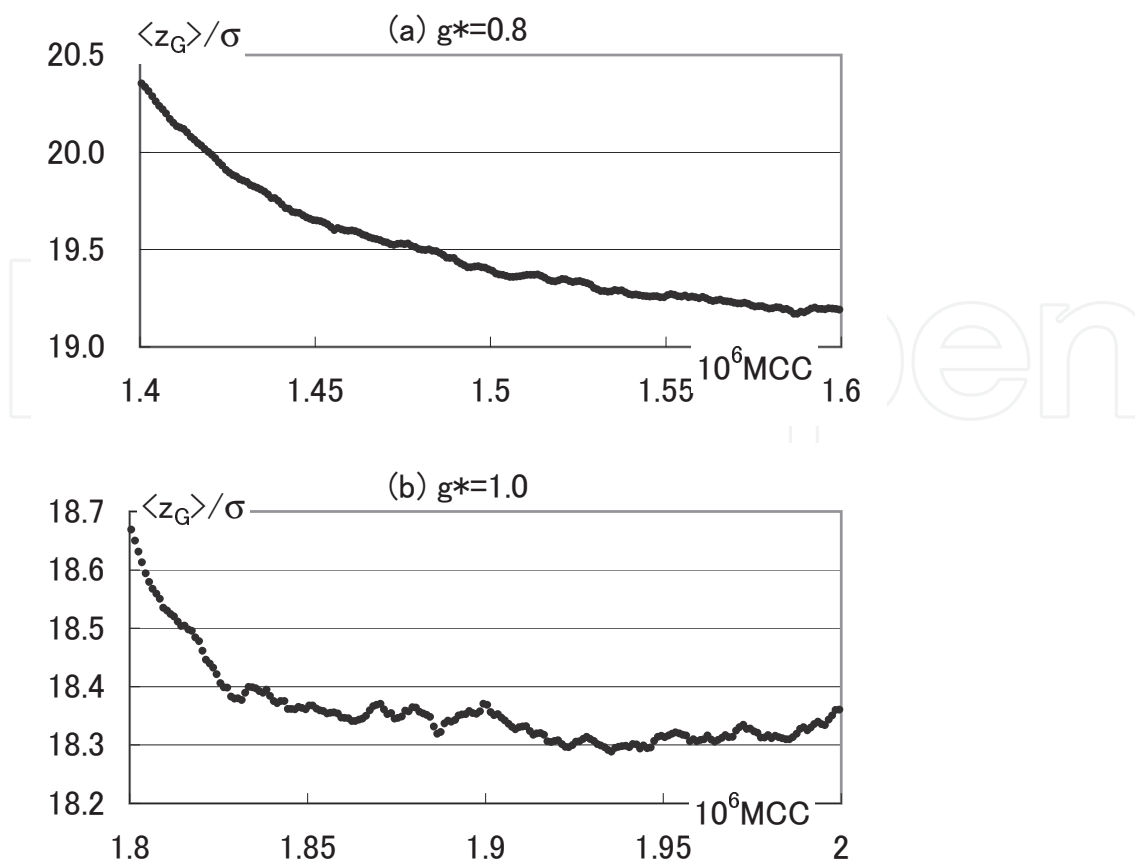


Fig. 7. Evolution of the center of gravity for 6656 hard spheres in a system with the square-patterned wall for a case that defect disappearance occurred at  $g^*$  lower than 0.9; during (a)  $g^* = 0.8$  and (b) 1.0. Running block average over  $10^3$  Monte Carlo cycles at every  $10^3$  Monte Carlo cycle is taken. Statistical errors are within  $0.011\sigma$  for (a) and  $0.008\sigma$  for (b).

sinking of the center of gravity during  $g^* = 1.0$  [Figure 9 (a)] to be of a single relaxation mode and a fluctuation around equilibrium as in a recent paper (Mori, in press). Unlike a recent paper (Mori, in press), the sinking during  $1.9-1.93 \times 10^6$  Monte Carlo cycle may be regarded as splitting a metastable state before this duration and an equilibrium state after that. However, as compared to Figure 9 (b) and the corresponding figure in a recent paper (Mori, in press), the multiple relaxation manner is not significant. Thus, the sinking of the center of the gravity during  $g^* = 1.0$  is of a single relaxation mode or of two stage manner with weak activation barrier between two stages. We can regard the sinking of the center of gravity in Figure 9 (b) to be a two stage manner; the system stay in a metastable equilibrium state during  $2.63-2.66 \times 10^6$  Monte Carlo cycle and then relaxes to an equilibrium state after  $2.75 \times 10^6$  Monte Carlo cycle. The two stage manner is more pronounced in a recent paper Mori (in press); the system stays in a metastable equilibrium state during  $2.63-2.71 \times 10^6$  Monte Carlo cycle and then relaxes to an equilibrium state after  $2.75 \times 10^6$  Monte Carlo cycle. An interesting thing is that despite shrinking of a "single" stacking fault is involved in Figure 6 (d) and Figure 8 (f), the sinking of the center of gravity in Figure 7 (b) and Figure 9 (b) is of a multiple manner. Of course, this is not surprising. Those behaviors are just similar to that in  $N = 1664$  small system with a flat bottom.

Figure 10 shows snapshots at  $g^* = 0.4-0.5$  and  $0.8-0.9$  for  $N = 26624$  system. Comparing  $xz$  projection of Figure 10 (a) and (b) we see that the splitting of the projection of lattice lines

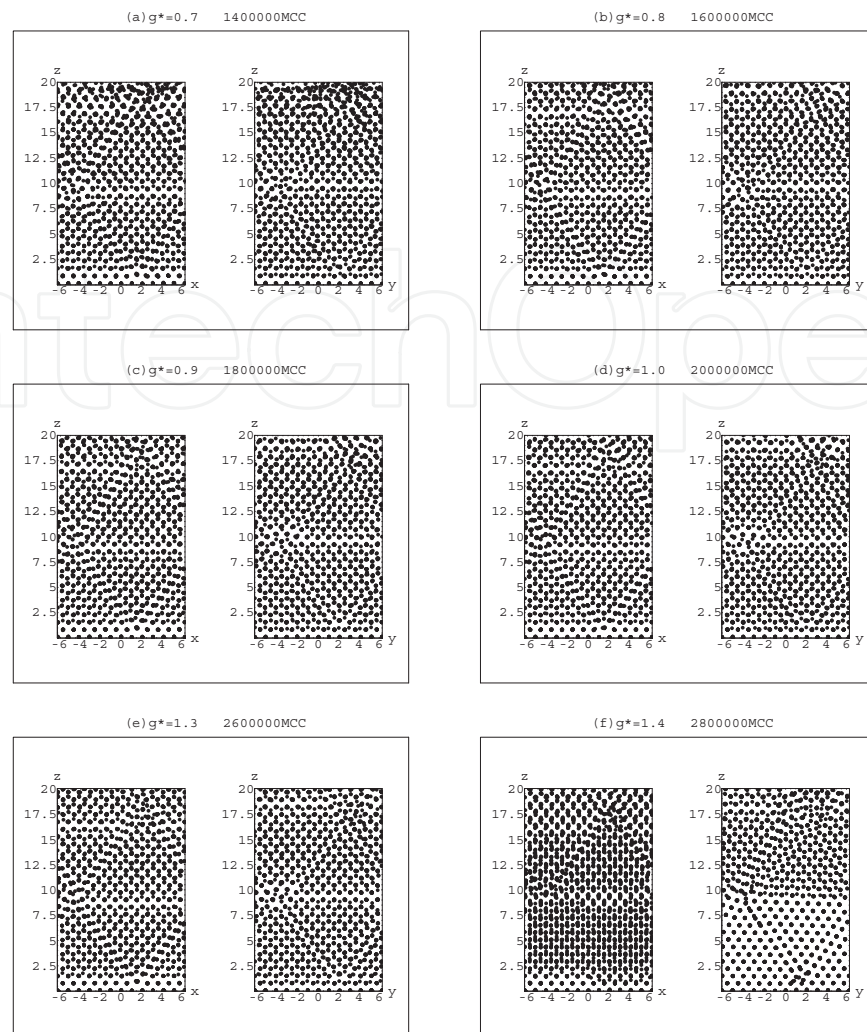


Fig. 8. Snapshot for 6656 hard spheres in a system with the square-patterned flat wall for a case that defect disappearance occurred at  $g^*$  higher than 0.9; at (a)  $g^* = 0.7$ , (b) 0.8, (c) 0.9, (d) 1.0, (e) 1.3, and (f) 1.4.

disappeared in portion  $3 < z^* < 10$ . This indicates shrinking of one or a few stacking faults running along  $(1\bar{1}1)$  or  $(1\bar{1}\bar{1})$  as discussed already. Comparing  $yz$  projection of Figure 10 (c) and (d) we see that the splitting of the projection of lattice lines disappeared in portion  $2.5 < z^* < 8$ . The splitting of the projection of lattice lines in  $xz$  direction has already disappeared at  $g^* = 0.8$ . This means shrinking of one or a few stacking faults running along  $(1\bar{1}1)$  or  $(1\bar{1}\bar{1})$  occurred. What is notable is the formation of triangular shapes both in  $xz$  and  $yz$  projections in Figure 10 (d). The suggestion of the stacking fault tetrahedron is as already discussed.

The evolutions of the center of gravity for  $N = 26624$  system during  $g^* = 0.5$  and 0.9 are plotted in Figure 9. During  $g^* = 0.5$  [Figure 11 (a)] the relaxation is of a single mode and has not reached to equilibrium yet. Figure 11 (a) is essentially the same as the corresponding figure in a recent paper (Mori, in press). Despite that the defect disappearance was proceeded, the system was not trapped into any metastable configuration. The activation barrier for the glide of dislocations or the motion of defect toward disappearance may become lower or vanishing as the system size becomes larger. Figure 11 (b) is quite similar to the corresponding figure

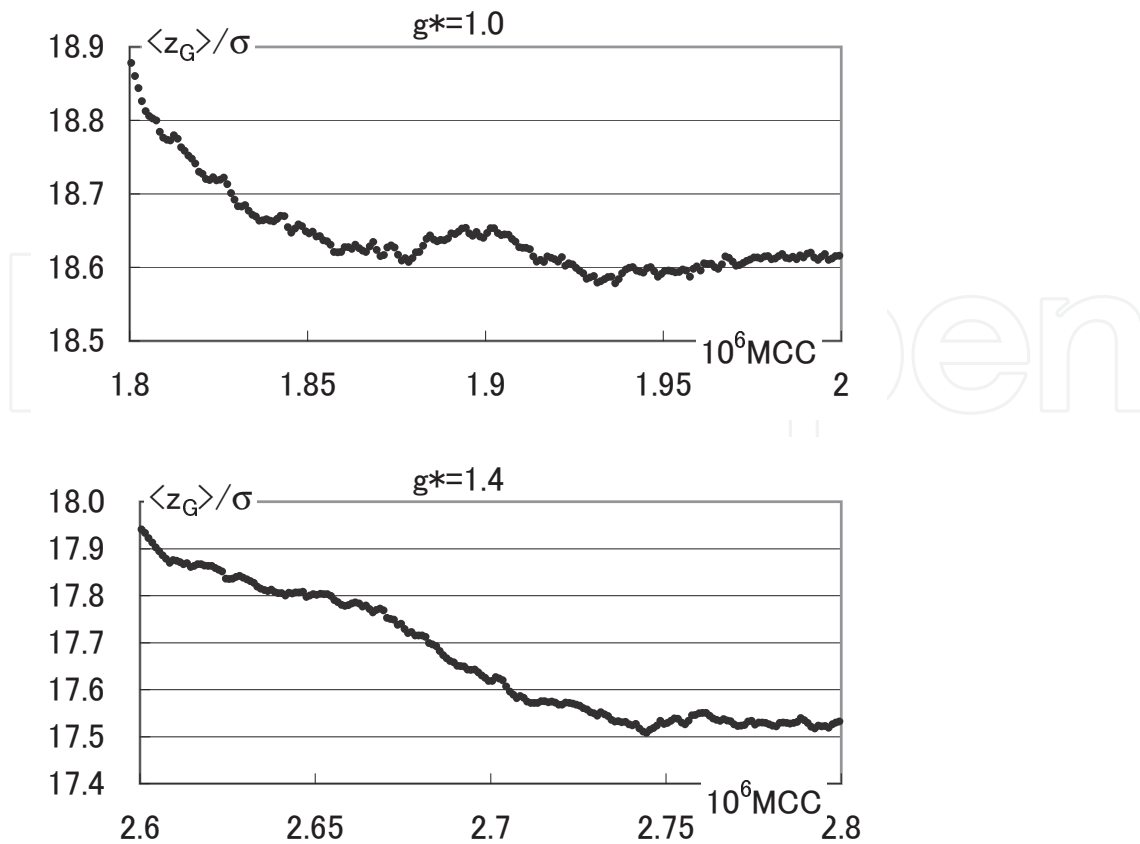


Fig. 9. Evolution of the center of gravity for 6656 hard spheres in a system with the square-patterned wall for a case that defect disappearance occurred at  $g^*$  higher than 0.9; during (a)  $g^* = 1.0$  and (b) 1.4. Running block average over  $10^3$  Monte Carlo cycles at every  $10^3$  Monte Carlo cycle is taken. Statistical errors are within  $0.010\sigma$  for (a) and  $0.007\sigma$  for (b).

in a recent paper (Mori, in press). It is of a single relaxation mode and fluctuation around equilibrium is observed.

## 5. Concluding remarks

We demonstrated the glide mechanism of a Shockley partial dislocation, which terminated an intrinsic stacking fault, for defect disappearance in hard-sphere colloidal crystal in fcc (001) stacking under gravity by Monte Carlo simulations (Mori et al., 2007a). This mechanism was seen at  $g^* \cong 0.9$  in a fcc (001) stacking crystal. Thus, we can say that we have pointed out a superiority of the colloidal epitaxy, which realizes the fcc (001) stacking.

However, the fcc (001) stacking in those simulations is forced by a stress from a small periodic boundary simulation box. That is, the driving force for the fcc (001) stacking was artificial. To resolve this shortcoming we have replaced the flat bottom wall with a square patterned one. By this mean, artificial driving force has been replaced with a realizable one. We have demonstrated the defect disappearance in those simulations.

In this chapter, we have concentrated on the defect disappearance and looked into the snapshot at relatively high  $g^*$ . Crystallization processes at low  $g^*$  have already been observed for the flat wall (Biben et al., 1994; Marechal & Dijkstra, 2007). Formation of a few crystalline layers at the bottom for the flat and square-patterned cases, details of which have been omitted

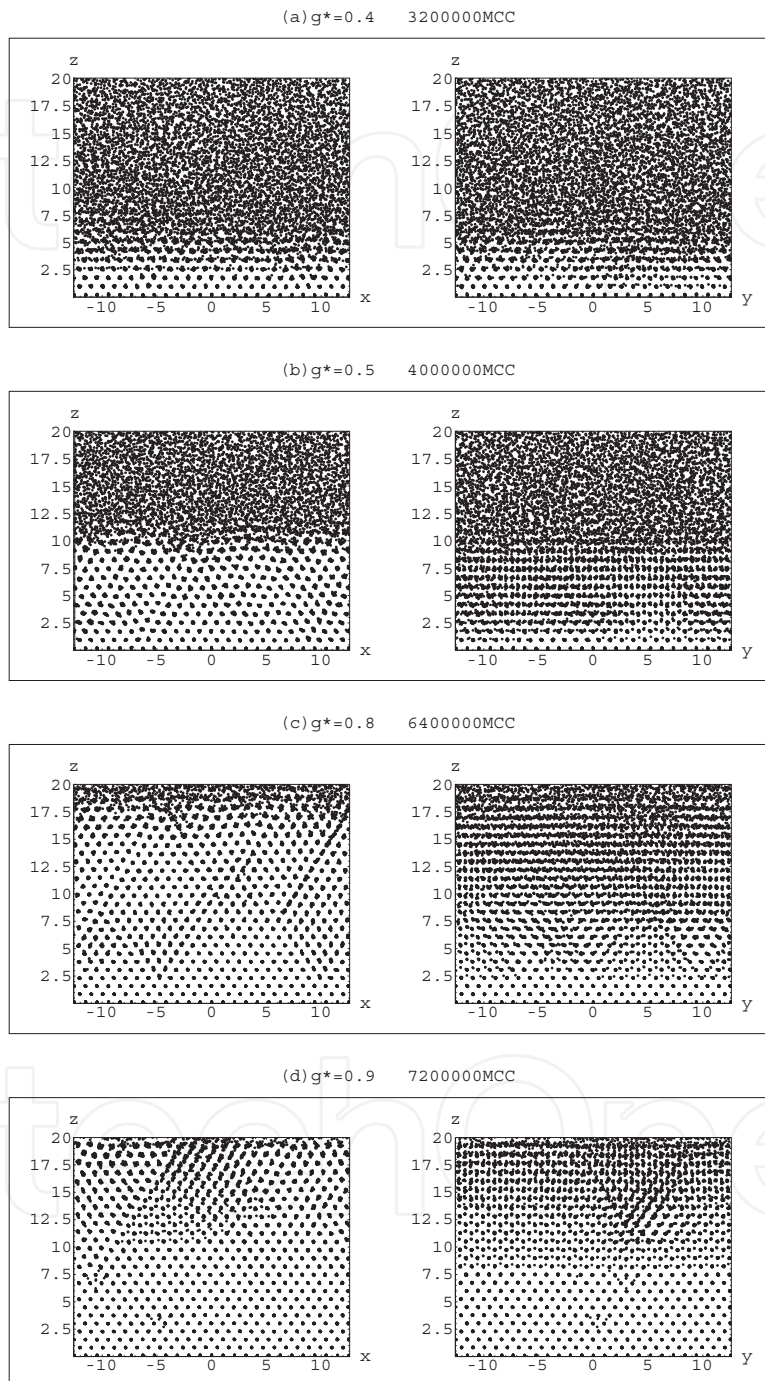


Fig. 10. Snapshot for 26624 hard spheres in a system with the square-patterned wall.

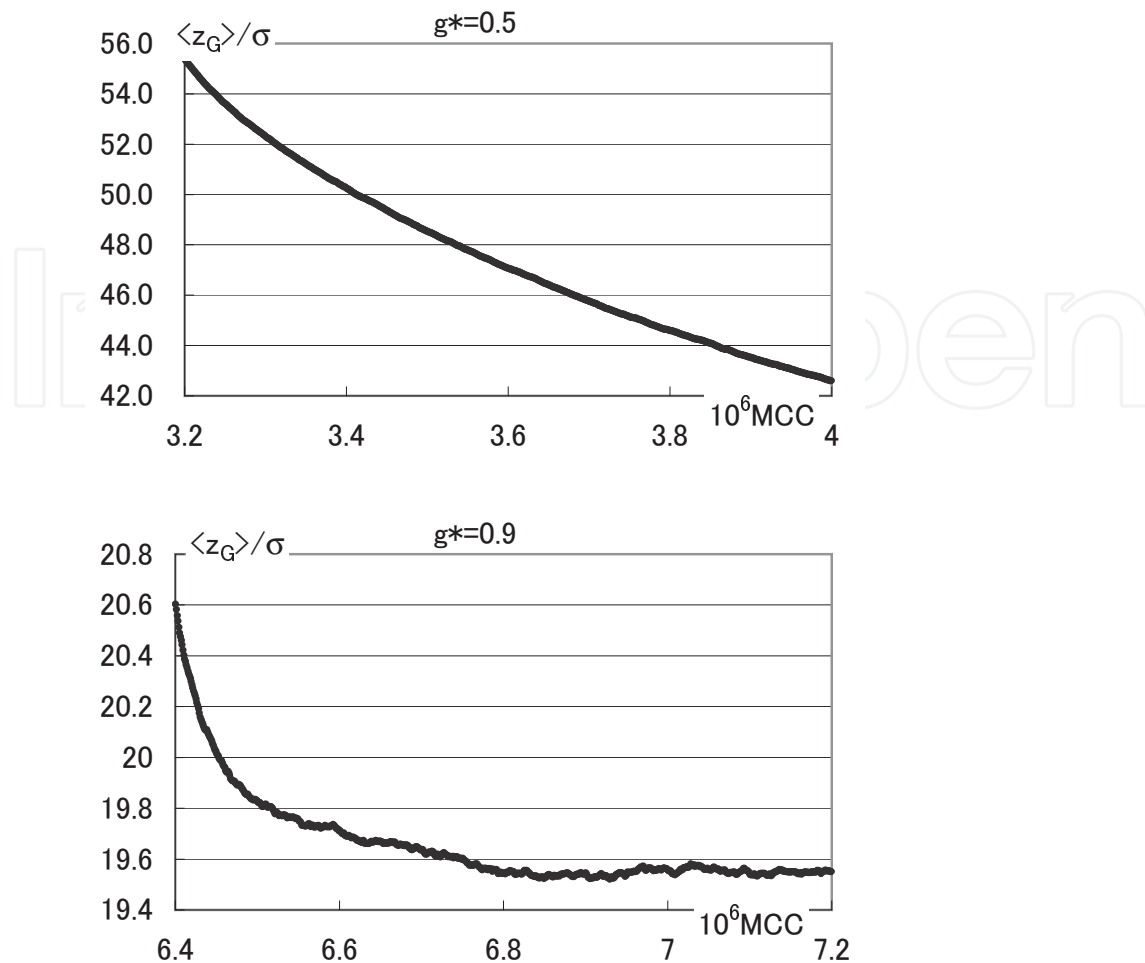


Fig. 11. Evolution of the center of gravity for 26624 hard spheres in a system with the square-patterned wall; during (a)  $g^* = 0.5$  and (b) 0.9. Running block average over  $10^3$  Monte Carlo cycles at every  $10^3$  Monte Carlo cycle is taken. Statistical errors are within  $0.0002\sigma$  for (a) and  $6 \times 10^5\sigma$  for (b).

in this chapter, is in agreement with the previous observation. More detailed analyses are in progress.

In simulations reported in this chapter, we adopted a conventional Monte Carlo method. Hence, the time corresponding to one Monte Carlo cycle varied. Indeed, acceptance ration varied depending on the density with a fixed maximum displacement of the Monte Carlo particle move. To perform kinetic Monte Carlo simulations to reproduce time evolution corresponding to real time is of interest. Also, molecular dynamics and Brownian dynamics simulations are planned.

## 6. References

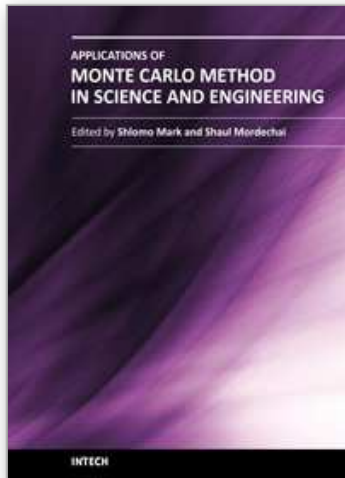
- Ackerson, B. J.; Paulin, S. E.; Johnson, B.; van Megen, W.; Underwood, S (1999). Crystallization by settling in suspension of hard spheres. *Physics Review E*, Vol. 59, No. 6, (June, 1999) 6903-6913, ISSN 1539-3755 (print), 1550-2376 (online), 1538-4519 (CD-Rom)
- Alder, B. J.; Wainwright, T. E. (1957). Phase Transition for a Hard Sphere System. *The Journal of Chemical Physics*, Vol. 27, No. 5, (November, 1957) 1208-1209, ISSN 0021-9606 (print), 1089-7690 (online)

- Antl, L.; Goodwin, J. W.; Hill, R. D.; Ottewill, R. H.; Owens, S. M.; Papworth, S. P.; Waters, J. A. (1986). The preparation of poly(methyl methacrylate) latices in non-aqueous media. *Colloids and Surfaces*, Vol. 17, No. 1, (January, 1986) 67-78, ISSN 0166-6622
- Biben, T.; Hansen, J.-P.; Barrat, J.-L. (1993). Density profiles of concentrated colloidal suspensions in sedimentation equilibrium. *The Journal of Chemical Physics*, Vol. 98, No. 9, (May, 1993) 7330-7344, ISSN 0021-9606 (print), 1089-7690 (online)
- Biben, T.; Ohnesorge, R.; Löwen, H. (1994). Crystallization in Sedimentation Profiles of Hard Spheres. *Europhysics Letters*, Vol. 28, No. 9, (December, 1994) 665-670, ISSN 0295-5075 (print), 1286-4854 (online)
- van Blaaderen, A.; Ruel, R.; Wiltzius, R. (1997). Template-directed colloidal crystallization. *Nature*, Vol. 385, No. 6614, (January, 1997) 321-324, ISSN 0028-0836 (print), 1476-4687 (online)
- Davidchack, R.; Laird, B. B. (1998). Simulation of the hard-sphere crystal-melt interface. *The Journal of Chemical Physics*, Vol. 108, No. 22, (June, 1998) 9452-9462, ISSN 0021-9606 (print), 1089-7690 (online)
- Hirth, J. H. & Loth, J. (1982). *Theory of Dislocations*, 2nd ed., Wiley, ISBN 0-89464-617-6, New York.
- Hoover, W. G.; Ree, F. H. (1968). Melting Transition and Communal Entropy for Hard Spheres. *The Journal of Chemical Physics*, Vol. 49, No. 8, (October, 1968) 3609-3617, ISSN 0021-9606 (print), 1089-7690 (online)
- John, S. (1987). Strong localization of photons in certain disordered dielectric superlattices. *Physical Review Letters*, Vol. 58, No. 23, (June, 1987) 2486-2489, ISSN 0031-9007 (print), 1079-7114 (online), 1092-0145 (CD-Rom)
- Kirkpatrick, S.; Gelatt, C. D.; Vecchi, P. (1983). Optimization by Simulated Annealing. *Science*, Vol. 220, No. 4598, (May, 1983) 671-680, ISSN 0036-8075 (print), 1095-9203 (online)
- Lin, K.-h.; Crocker, J. C.; Parasad, V.; Shofield, A.; Weitz, D. A.; Lubensky, T. C.; Yodh, Y. G. (2000). Entropically Driven Colloidal Crystallization on Patterned Surfaces. *Physical Review Letters*, Vol. 85, No. 8, (August, 2000) 1770-1773, ISSN 0031-9007 (print), 1079-7114 (online), 1092-0145 (CD-Rom)
- Lyubartev, A. P.; Martsinovski, A. A.; Shevkunov, S. V.; Vorontsov-Velyaminov, P. N. (1992). New approach to Monte Carlo calculation of the free energy: Method of expanded ensembles. *The Journal of Chemical Physics*, Vol. 96, No. 3, (February, 1992) 1776-1783, ISSN 0021-9606 (print), 1089-7690 (online)
- Marechal, M.; Dijkstra, M. (2007). Crystallization of colloidal hard spheres under gravity. *Physical Review E*, Vol. 75, No. 6, (June, 2007) 061404-1-061404-8, ISSN 1539-3755 (print), 1550-2376 (online), 1538-4519 (CD-Rom)
- Marinari, E.; Parisi, G. (1992). Simulated Tempering: A New Monte Carlo Scheme. *Europhysics Letters*, Vol. 19, No. 6, (July, 1992) 451-458, ISSN 0295-5075 (print), 1286-4854 (online)
- Megens, M.; van Kats, C. M.; Bösecke, P.; Vos, W. L. (1997). Synchrotron small-angle X-ray scattering of colloids and photonic colloidal crystal. *Journal of Applied Crystallography*, Vol. 30, No. 5-2, (October, 1997) 637-641, ISSN 0021-8891 (print), ISSN 1600-5767 (online)
- Mori, A.; Manabe, R.; Nishioka, K. (1995). Construction and investigation of a hard-sphere crystal-melt interface by a molecular dynamics simulation. *Physical Review E*, Vol. 51, No. 5, (May, 1995) R3831-R3833, ISSN 1539-3755 (print), 1550-2376 (online), 1538-4519 (CD-Rom)

- Mori, A.; Yanagiya, S.-i.; Suzuki, Y.; Sawada, T.; Ito, K. (2006). Crystal structure of hard spheres under gravity by Monte Carlo simulation. *Science and Technology of Advanced Materials*, Vol. 7, No. 3, (April, 2006) 296-302, ISSN 1468-6996
- Mori, A.; Yanagiya, S.-i.; Suzuki, Y.; Sawada, T.; Ito, K. (2006). Monte Carlo simulation of crystal-fluid coexistence states in the hard-sphere system under gravity with stepwise control. *The Journal of Chemical Physics*, Vol. 124, No. 17, (May, 2006) 174507-1-174507-10, ISSN 0021-9606 (print), 1089-7690 (online)
- Mori, A.; Suzuki, Y.; Yanagiya, S.-i.; Sawada, T.; Ito, K. (2007). Shrinking stacking fault through glide of the Shockley partial dislocation in hard-sphere crystal under gravity. *Molecular Physics*, Vol. 105, No. 10, (May, 2007) 1377-1383, ISSN 0026-8976 (print), 1362-3028 (online); errata *ibid.* Vol. 106, No. 1, (January, 2008) 187-187
- Mori, A.; Suzuki, Y.; Yanagiya, S.-i. (2007). Succession of stacking disorder in hard-sphere crystal under gravity by Monte Carlo simulation. *Fluid Phase Equilibria*, Vol. 257, No. 2, (August, 2007) 131-138, ISSN 0378-3812
- Mori, A.; Suzuki, Y.; Matsuo, S. (2009). Disappearance of a Stacking Fault in Hard-Sphere Crystals under Gravity. *Progress of Theoretical Physics Supplement*, Vol. 178, (April, 2009) 33-40, ISSN 0375-9687 (print), 1347-0481 (online)
- Mori, A.; Suzuki, Y. (2010). Interplay between elastic fields due to gravity and a partial dislocation for a hard-sphere crystal coherently grown under gravity: driving force for defect disappearance. *Molecular Physics*, Vol. 108, No. 13, (July, 2010) 1731-1738, ISSN 0026-8976 (print), 1362-3028 (online)
- Mori, A. (in press). Monte Carlo simulation of growth of hard-sphere crystals on a square pattern. *Journal of Crystal Growth*, in press, ISSN 0022-0248
- Ohtaka, K. (1979). Energy band of photons and low-energy photon diffraction. *Physical Review B*, Vol. 19, No. 10, (May, 1979) 5057-5067, 1098-0121 (print), 1550-235X (online), 1538-4489 (CD-Rom)
- Paulin, S. E.; Ackerson, B. J. (1990). Observation of a phase transition in the sedimentation velocity of hard spheres. *Physical Review Letters*, Vol. 64, No. 22, (May, 1990) 2663-2666, ISSN 0031-9007 (print), 1079-7114 (online), 1092-0145 (CD-Rom); errata *ibid.*, Vol. 65, No. 5, (July, 1990) 668-668
- Phan, S. E.; Russel, W. B.; Cheng, Z.; Zhu, J.; Chaikin, P. M.; Dunsmur, J. H.; Ottewill, R. H. (1996). Phase transition, equation of state, and limiting shear viscosities of hard sphere dispersions. *Physical Review E*, Vol. 54, No. 6, (December, 1996) 6633-6645, ISSN 1539-3755 (print), 1550-2376 (online), 1538-4519 (CD-Rom)
- Pusey, P. N.; van Megen, W. (1986). Phase behaviour of concentrated suspensions of nearly hard colloidal spheres. *Nature*, Vol. 320, No. 6060, (March, 1986) 340-342, ISSN 0028-0836 (print), 1476-4687 (online)
- Pusey, P. N.; van Megen, W.; Bartlett, R.; Ackerson, B. J.; Parity, J. G.; Underwood, S. M. (1989). Structure of crystals of hard colloidal spheres. *Physical Review Letters*, Vol. 63, No. 25, (December, 1989) 2753-2756, ISSN 0031-9007 (print), 1079-7114 (online), 1092-0145 (CD-Rom)
- Suzuki, Y.; Sawada, T.; Mori, A.; Tamura, K. (1989). Colloidal Crystallization by Centrifugation. *Kobunsh Ronbumshu*, Vol. 64, No. 3, (March, 2007) 161-165 [in Japanese], ISSN 1881-5685 (print), 0386-2186 (online)
- Underwood, S. M.; Taylor, J. R.; van Megen, W. (1994). Sterically Stabilized Colloidal Particles as Model Hard Spheres. *Langmuir*, Vol. 10, No. 10, (October, 1994) 3550-3554, IPrint Edition ISSN 0743-7463, Web Edition ISSN 1520-5827

- Wadachi, M.; Toda, M. (1972). An Evidence for the Existence of Kirkwood-Alder Transition. *Journal of the Physical Society of Japan*, Vol. 32, No. 4, (April, 1972) 1147-1147, ISSN 0031-9015 (print), 1347-4073 (online)
- Wood, W. W.; Jacobson, J. D. (1957). Preliminary Results from a Recalculation of the Monte Carlo Equation of State of Hard Spheres. *The Journal of Chemical Physics*, Vol. 27, No. 5, (November, 1957) 1207-1208, ISSN 0021-9606 (print), 1089-7690 (online)
- Yablonovitch, E. (1987). Inhibited Spontaneous Emission in Solid-State Physics and Electronics. *Physical Review Letters*, Vol. 58, No. 20, (May, 1987) 2059-2062, ISSN 0031-9007 (print), 1079-7114 (online), 1092-0145 (CD-Rom)
- Yanagiya, S.-i.; Mori, A.; Suzuki, Y.; Miyoshi, Y.; Kasuga, M.; Sawada, T.; Ito, K.; Inoue, T. (2005). Enhancement of Crystallization of Hard Spheres by Gravity: Monte Carlo Simulation. *Japanese Journal of Applied Physics*, Part. 1, Vol. 44, No. 7A, (July, 2005) 5113-5116, ISSN 0021-4922 (print), 1347-4065 (online)
- Zhu, J.; Li, M.; Rogers, R.; Meyer, W.; Ottewill, R, STS-73 Space Shuttle Crew; Russel, W.; Chaikin, P. M. (1997). Crystallization of hard-sphere colloids in microgravity. *Nature*, Vol. 387, No. 6636, (June, 1997) 883-885, ISSN 0028-0836 (print), 1476-4687 (online)

IntechOpen



## **Applications of Monte Carlo Method in Science and Engineering**

Edited by Prof. Shaul Mordechai

ISBN 978-953-307-691-1

Hard cover, 950 pages

**Publisher** InTech

**Published online** 28, February, 2011

**Published in print edition** February, 2011

In this book, Applications of Monte Carlo Method in Science and Engineering, we further expose the broad range of applications of Monte Carlo simulation in the fields of Quantum Physics, Statistical Physics, Reliability, Medical Physics, Polycrystalline Materials, Ising Model, Chemistry, Agriculture, Food Processing, X-ray Imaging, Electron Dynamics in Doped Semiconductors, Metallurgy, Remote Sensing and much more diverse topics. The book chapters included in this volume clearly reflect the current scientific importance of Monte Carlo techniques in various fields of research.

### **How to reference**

In order to correctly reference this scholarly work, feel free to copy and paste the following:

Atsushi Mori (2011). Monte Carlo Simulations on Defects in Hard-Sphere Crystals Under Gravity, Applications of Monte Carlo Method in Science and Engineering, Prof. Shaul Mordechai (Ed.), ISBN: 978-953-307-691-1, InTech, Available from: <http://www.intechopen.com/books/applications-of-monte-carlo-method-in-science-and-engineering/monte-carlo-simulations-on-defects-in-hard-sphere-crystals-under-gravity>

**INTECH**  
open science | open minds

### **InTech Europe**

University Campus STeP Ri  
Slavka Krautzeka 83/A  
51000 Rijeka, Croatia  
Phone: +385 (51) 770 447  
Fax: +385 (51) 686 166  
[www.intechopen.com](http://www.intechopen.com)

### **InTech China**

Unit 405, Office Block, Hotel Equatorial Shanghai  
No.65, Yan An Road (West), Shanghai, 200040, China  
中国上海市延安西路65号上海国际贵都大饭店办公楼405单元  
Phone: +86-21-62489820  
Fax: +86-21-62489821

© 2011 The Author(s). Licensee IntechOpen. This chapter is distributed under the terms of the [Creative Commons Attribution-NonCommercial-ShareAlike-3.0 License](#), which permits use, distribution and reproduction for non-commercial purposes, provided the original is properly cited and derivative works building on this content are distributed under the same license.

IntechOpen

IntechOpen